Global Change Biology

Global Change Biology (2010), doi: 10.1111/j.1365-2486.2009.02157.x

Robust dynamics of Amazon dieback to climate change with perturbed ecosystem model parameters

BENJAMIN POULTER*†, FRED HATTERMANN†, ED HAWKINS‡, SÖNKE ZAEHLE§, STEPHEN SITCH¶, NATALIA RESTREPO-COUPE‖, URSULA HEYDER† and WOLFGANG CRAMER†

*Swiss Federal Research Institute WSL, Zürcherstrasse 111, 8903 Birmensdorf, Switzerland, †Potsdam Institute for Climate Impact Research (PIK), Telegraphenberg A26, D-14412 Potsdam, Germany, ‡Department of Meteorology, University of Reading, Reading RG6 6BB, UK, §Max Planck Institute for Biogeochemistry, PO Box 100164, 07701 Jena, Germany, ¶School of Geography, University of Leeds, Leeds LS2 9JT, UK, ‖Department of Ecology and Evolutionary Biology, University of Arizona, Tucson, AZ 85721, USA

Abstract

Climate change science is increasingly concerned with methods for managing and integrating sources of uncertainty from emission storylines, climate model projections, and ecosystem model parameterizations. In tropical ecosystems, regional climate projections and modeled ecosystem responses vary greatly, leading to a significant source of uncertainty in global biogeochemical accounting and possible future climate feedbacks. Here, we combine an ensemble of IPCC-AR4 climate change projections for the Amazon Basin (eight general circulation models) with alternative ecosystem parameter sets for the dynamic global vegetation model, LPJmL. We evaluate LPJmL simulations of carbon stocks and fluxes against flux tower and aboveground biomass datasets for individual sites and the entire basin. Variability in LPJmL model sensitivity to future climate change is primarily related to light and water limitations through biochemical and water-balance-related parameters. Temperature-dependent parameters related to plant respiration and photosynthesis appear to be less important than vegetation dynamics (and their parameters) for determining the magnitude of ecosystem response to climate change. Variance partitioning approaches reveal that relationships between uncertainty from ecosystem dynamics and climate projections are dependent on geographic location and the targeted ecosystem process. Parameter uncertainty from the LPJmL model does not affect the trajectory of ecosystem response for a given climate change scenario and the primary source of uncertainty for Amazon 'dieback' results from the uncertainty among climate projections. Our approach for describing uncertainty is applicable for informing and prioritizing policy options related to mitigation and adaptation where long-term investments are required.

Keywords: climate change, forest dieback, Latin hypercube, photosynthesis, variance partitioning, vegetation dynamics, water-use

Received 6 February 2009 and accepted 8 November 2009

Introduction

Climate change research is increasingly concerned with quantifying carbon cycle feedbacks, their probability, and ecological impacts in the context of setting mitigation and adaptation policy (Friedlingstein *et al*., 2003; Cox & Stephenson, 2007; Sitch *et al*., 2008). These issues are especially relevant in tropical ecosystems where changes in carbon fluxes and stocks may have disproportionately larger effects on global biogeochemistry and climate than in other regions (Cox *et al*., 2004; Raddatz *et al*., 2007; Bonan, 2008; Sitch *et al*., 2008). The Amazon Basin, for example, is categorized as a terrestrial biogeochemical 'hotspot' where climate change and deforestation may lead to massive losses of carbon that acts as a positive feedback to rising atmospheric CO_2 concentrations (Cox *et al*., 2008; Lenton *et al*., 2008; Nepstad *et al*., 2008). The probability of climate change driven Amazon 'dieback' (i.e., the rapid change in vegetation cover, from forest to nonforest, which may include the release of Amazon forest carbon stocks to the atmosphere) remains a subject of much debate within the climate and vegetation modeling community, in part because of the range of sensitivity of ecosystem model responses to drought but also due to the wide range of projected climate scenarios for South America (Salazar *et al*., 2007; Li *et al*., 2008; Sitch *et al*., 2008).

The temporal and spatial dynamics of future carbon cycle feedbacks remain for the most part, probabilistic, because they accumulate uncertainty from multiple

Correspondence: Benjamin Poulter, tel. +41 44 739 21 11, fax +41 44 739 22 15, e-mail: Benjamin.Poulter@wsl.ch

sources ranging from greenhouse gas emission storylines (Nakicenovic, 2000), variations between climate sensitivity of general circulation models (GCMs) (Li *et al.*, 2006), and differences among the parameterization of terrestrial ecosystem models (Cramer *et al.*, 2001). Within these primary sources of uncertainty exists differences between process formulations that vary among models and their representation of earth system dynamics. Beyond the level of 'first principles,' where processes are governed by well-established physical laws, many parameters and processes include uncertainty because of their different theoretical and empirical foundations, for example, relating leaf respiration to a Q_{10} function vs. leaf nitrogen content. Variability is also inherent to ecological systems, resulting from genetic or phenotypic variation and may often be overlooked in modeling because of the necessity to generalize certain concepts within a hypothesis testing framework, such as the concept of plant functional types (PFTs) (Prentice *et al.*, 2007). In this context, climate impact science generally proceeds within a risk assessment framework to inform management and policy decisions related to adaptation and mitigation (Jones, 2001; Cox & Stephenson, 2007).

Constraining parameter and process uncertainty within climate and vegetation models is challenging in tropical regions because of the complexity of ecosystem–climate feedbacks (Werth & Avissar, 2004) and the diversity and abundance of tropical plant species and their functional traits (Reich, 1995). Tropical climate projections from atmospheric GCMs vary widely, with some models representing 20th century climate patterns more realistically than others (Li *et al.*, 2006). Observational data (i.e., remote sensing and field inventories) that might be used for model calibration and evaluation are often problematic, because of their coarse spatial resolution or limited spatial coverage of field sites (Phillips *et al.*, 2002). Remote sensing and eddy covariance data may also be biased because of the presence of seasonal cloud cover or atmospheric stability problems (Saleska *et al.*, 2003; Kobayashi & Dye, 2005). Tropical aboveground biomass and carbon fluxes can be strongly influenced by site specific disturbance histories (Friend *et al.*, 2007), soil nutrient status (e.g., the presence of 'terra preta' soils) and hydrologic conditions (i.e., terra firme uplands vs. seasonally inundated floodplain forests) that are not represented in regional to global scale models.

Probabilistic modeling can utilize and integrate these sources of uncertainty by using model variance partitioning and signal-to-noise ratio approaches to better quantify the robustness of projected ecosystem change. An improved understanding of the relative contribution of model parameters to uncertainty can also help guide data assimilation approaches to estimate model parameters and better target future field research objectives. There are many examples of earth system model uncertainty analysis that have focused on ecosystem model parameter uncertainty (Hallgren & Pitman, 2000; Zaehle *et al.*, 2005; Wramneby *et al.*, 2008; Xu *et al.*, 2009), process formulation (Huntingford *et al.*, 2008; Galbraith D, Huntingford C, Cox PM, Levy PE, Sitch S, Meir P, Williams M, unpublished results), and climate projection variability (Zaehle *et al.*, 2007) including coupled vegetation-climate dynamics (Alton *et al.*, 2007). However, few approaches have explicitly examined the combination of vegetation model uncertainty in the context of climate projection ensemble variability.

The objectives of this paper are to evaluate the spatiotemporal dynamics of ecosystem parameter importance to 21st century climate change using the LPJmL dynamic global vegetation model (DGVM) (Sitch *et al.*, 2003; Bondeau *et al.*, 2007). We approach this problem by focusing on the importance of LPJmL parameters using Latin hypercube sampling methods and Monte Carlo simulations in a two-stage process. First, we compared simulated output against observations for six tropical flux tower locations. This analysis identified the most important ecosystem model parameters responsible for simulation uncertainty. In the second stage, we conducted basin-wide simulations with climate data from eight GCMs to investigate the uncertainty of tropical ecosystem dynamics from the year 2000 to 2100. These simulations identified the relative importance of parameters controlling changes in carbon and vegetation dynamics, and provided the basis for partitioning uncertainty between LPJmL and the GCM ensemble.

Materials and methods

LPJmL model description

For this study, we used the LPJmL DGVM modified to include cropland dynamics (Sitch *et al.*, 2003; Bondeau *et al.*, 2007). This version also includes an updated hydrologic cycle (Gerten *et al.*, 2004) and modifications to leaf 'dark' respiration to represent the formulation presented in Haxeltine & Prentice (1996a). Additional changes also include (1) changes to tropical drought deciduous (TrRG) phenology, whereby TrRG drop leaves only due to moisture stress and (2) the lowering of maximum establishment rate for seedlings from 0.24 to 0.12 individuals per square meter. Both changes were implemented to stabilize vegetation and carbon dynamics and we explore their significance with their inclusion in the Latin hypercube parameter set (described in 'Parameter selection approach').

LPJmL estimates daily photosynthesis and transpiration for nine PFTs that are distinguished by their photosynthetic pathway (C_3 or C_4), physiognomy (woody or herbaceous), and phenology (deciduous or evergreen). Carbon is allocated to

Table 1 Site names and vegetation characteristics from LBA-MIP, the number in the first column corresponds with location on Fig. 1

Site name	Latitude, Longitude	Flux tower	Vegetation type (undisturbed)	Dry season length (months <100 mm ppt)
1. Manaus KM34	2°36′35.99″S 60°12′36″W	X	Evergreen broadleaf forest	2.1
2. Rebio Jaru Forest, Ji Parana (Tower A)	10°4′48″S 61°55′47″W	X	Evergreen broadleaf forest	4.5
3. Santarém KM67	2°51′35″S 54°57′36″W	X	Evergreen broadleaf forest	5.4
4. Santarém KM84	3°01′04″S 54°53′39″W	X	Evergreen broadleaf forest	5.4
5. Bananal Island	9°49′12″S 50°9′35″W	X	Evergreen broadleaf forest	5.5
6. Sao Paulo Cerrado (Pé-de-Gigante Reserve)	21°37′12″S 47°38′59″W	X	Cerrado	5.9

LBA-MIP, Large Scale Biosphere Atmosphere Model Intercomparison Project.

various above and belowground pools and competition between individuals occurs for light and water. A fire disturbance module simulates consumption of biomass and resulting mortality (Thonicke *et al*., 2001). The LPJ-DGVM framework has been extensively validated at global scales (Sitch *et al*., 2003) and for temperate and boreal regions (Hickler *et al*., 2006), this study is the among first to evaluate LPJ against tropical flux tower data.

Two sets of model simulations were performed. The first focused on evaluating LPJmL against flux tower measurements and observed climate, selected along a precipitation gradient (Table 1) with a full set of 41 perturbed parameters ('Parameter selection approach'). The second analysis evaluated entire Amazon Basin-wide responses with a subset of these parameters to an ensemble of climate change projections. We confined our analysis to the spatial and temporal patterns of LPJmL outputs for carbon stocks and fluxes for the flux tower comparison and to carbon stocks and plant cover for the basin-wide simulations. The model simulations ('Datasets and Simulation Protocol') included ecological effects from the wildfire disturbance module, and focused on the natural dynamics of Amazonian forests. Although cropland dynamics are an important feature of tropical land cover change, there is large uncertainty of their intensity and spatial patterns into the future (Soares-Filho *et al*., 2006; Walker *et al*., 2009; Poulter *et al*., In press). Here, we focused our analysis on the primary driver related to the Amazon dieback phenomenon, which is climate-driven changes in precipitation and temperature (Cox *et al*., 2004).

Parameter selection approach

We identified a set of 41 parameters used in modeling ecosystem processes in LPJmL and affecting the carbon and water cycle, and vegetation dynamics (Table S1). These parameters were selected by combining literature review with an *a priori* focus on additional parameters considered important for tropical regions. We relied on several previous studies that have evaluated parameter uncertainty and their ranges for LPJ and the related BIOME model (Hallgren & Pitman, 2000; Zaehle *et al*., 2005; Wramneby *et al*., 2008). Similar model–data comparisons have identified canopy and belowground processes as a priority for realistically modeling tropical ecosystems (Saleska *et al*., 2003). To address these findings, we included parameters affecting leaf fall (i.e. leaf longevity and a soil moisture threshold for leaf abscission). For belowground processes, we explored parameter uncertainty for soil depth and rooting distributions described for various ecosystem types in Amazonia (Poulter *et al*., 2009b). For most parameters, their range was determined from literature values (rather than optimization, e.g., see Trudinger *et al*., 2007) and represented by a β-distribution: however, a uniform distribution was used when little to no justification for a central value existed (Table S1).

As in Zaehle *et al*. (2005), Latin hypercube sampling (McKay *et al*., 1979) was used to generate parameter sets for the flux tower comparison (1000 sets) and the basin-wide simulations (200 sets). The Latin hypercube sampling approach is designed to create a distribution of collections of parameters while accounting for previously sampled parameter values. In order to fully cover the hyper-dimensional parameter space it is recommended that at least 1.5–10 times the number of parameters are sampled (Saltelli & Tarantola, n.d.). For the site-level simulations, 1000 sets were generated for 41 parameters and for the basin-wide simulations, a reduced set of 21 parameters were selected with 200 sets generated (see 'Estimating parameter importance' for description of reduced set and its selection) (Table 2).

Datasets and simulation protocol

For the flux tower comparison, we used climate data for six locations provided by the Large Scale Biosphere Atmosphere

Table 2 List of parameters, original value, and parameter ranges, used in basin-wide simulations

Parameter name	Units	Main process	Original value	Latin hypercube distribution	Lower estimate	Upper estimate	Reference
Lower soil depth	M	Hydrology	1000	Uniform	300	10 000	Poulter *et al.* (2009b)
Maximum evapotranspiration rate (TrRG)	mm day^{-1}		7	Beta*	4	8	Hallgren & Pitman (2000)
Maximum evapotranspiration rate (TrEV)			7		3	7.5	
Maximum establishment rate	# per m^2	Vegetation dynamics	0.12		0.05	0.48	Dolman *et al.* (1991)
Rooting distribution (TrRG)	Fraction	Allocation	0.6	Uniform	0.6	1	Poulter *et al.* (2009b)
Rooting distribution (TrEV)			0.85		0.6	1	
Leaf longevity threshold for raingreens	Days		365	Beta*	120	365	Reich (1995)
Leaf to root biomass ratio under nonwater-stressed conditions (TrRG)	Fraction		1		0.85	1.15	No reference (15% CV)†
Albedo	Unit-less	Photosynthesis	0.17		0.08	0.17	Bonan (2008)
Leaf respiration as a fraction of Rubisco capacity in C_3 plants			0.015		0.01	0.021	Farquhar *et al.* (1980), Hallgren & Pitman (2000)
Sapwood turnover (TrRG)	Years		20		5	100 (60)	Bartelink (1998)
Sapwood turnover (TrEV)			20		5	100 (60)	
Leaf turnover (TrEV)			2		1 (2)	8	Reich (1995)
Intrinsic quantum efficiency of CO_2 uptake in C_3 plants	Unit-less		0.08		0.02 (0.05)	0.125	Hallgren & Pitman (2000), Farquhar *et al.* (1980)
Intrinsic quantum efficiency of CO_2 uptake in C_4 plants			0.053		0.03	0.054	
Photosynthesis scaling parameter (TrRG)			0.5		0.3	0.7	Haxeltine & Prentice (1996a)
Photosynthesis scaling parameter (TrEV)			0.5		0.3	0.7	
Photosynthesis co-limitation shape parameter (θ)			0.7		0.2	0.996	Collatz *et al.* (1991)
Light extinction coefficient			0.5		0.4 (0.5)	0.9	Shuttleworth (1988)
Specific leaf area (TrRG)	m^2 g^{-1} C	Allocation	0.5		0.35	0.65	No reference (30% CV)†
Specific leaf area (TrEV)			2		1.4	2.6	

TrEV and TrRG refer to the tropical evergreen and tropical raingreen plant function types used in LPJ, respectively.
*Beta distribution (where $\alpha = 2$ and $\beta = 2$).
†Benchmarked parameters in parentheses.

 Global Change Biology, doi: 10.1111/j.1365-2486.2009.02157.x

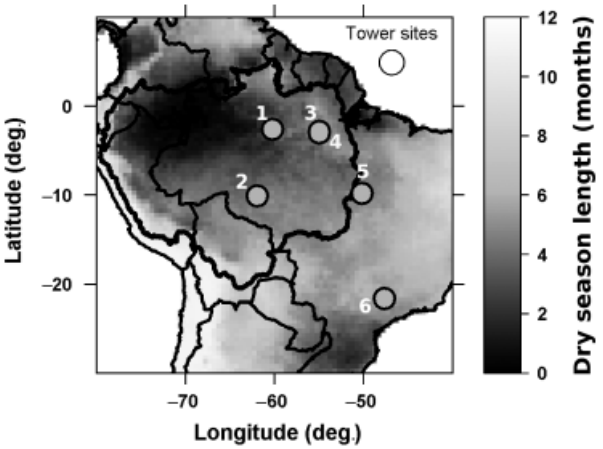

Fig. 1 Map of Amazon Basin and flux tower sites evaluated in this study. The dry season lengths are computed from TRMM satellite data (Poulter & Cramer, 2009) and show the mean of the years 1998–2008.

Table 3 Selected global climate models used in this study

	2095–2100	
Model	Delta precipitation	Delta temperature
CSIRO MK 3.0	−4.42	3.90
GFDL CM 2.1	−0.08	4.59
GISS Model E-R	15.27	3.62
IPSL CM4	44.64	4.09
MPI ECHAM 5.0	−0.16	5.45
NCAR PCM1	14.6	2.29
UKMO HadCM3	−28.94	7.15
UKMO HadGEM	−11.89	5.44

Simulations were performed at 1° spatial resolution starting in the year 1901 and ending in 2098. The emissions storyline was the SRES A2 scenario. Units are change from 1990 baseline, in percent (%) for delta precipitation and °C for temperature.

Model Intercomparison Project (LBA-MIP) as input for LPJmL simulations (da Rocha *et al*., 2009). The six sites were natural tropical forest stands (Fig. 1) where dry season length (number of months with <100 mm precipitation) ranged from 2.1 to 5.9 months. Hourly observed climate data (temperature, precipitation, and incoming shortwave solar radiation) were aggregated to monthly mean daily values. Incoming shortwave radiation was converted to percent cloud cover using equations from Haxeltine & Prentice (1996a). To extend the climatology from site years to a full 20th century simulation we normalized the Climatic Research Unit (CRU) climate dataset (New *et al*., 2002; Österle *et al*., 2003) to the monthly site data so that simulations began in the year 1901, following methods similar to Zaehle *et al*. (2005). Site specific soil texture data were related to their corresponding FAO soil type (Zobler, 1986) and global concentrations of atmospheric CO_2 used to represent site conditions from the CDIAC database (Keeling & Whorf, 2005).

The basin-wide simulations used data from eight GCMs involved with the IPCC Fourth Assessment Report (Table 3). These GCMs have been evaluated against various climate observations for the Amazon Basin (i.e., long-term trends in precipitation) and shown to simulate realistic 20th century climate, and also provide a wide range of future temperature and precipitation changes resulting in high GCM model uncertainty (Fig. 2; Li *et al*., 2006, 2008; Reichler & Kim, 2008). The climate model data (monthly precipitation, temperature, and percent cloud cover) were resampled from their original spatial resolution to a regular 1° resolution grid using bilinear interpolation and bias corrected using an anomaly approach (Malhi *et al*., 2009a). This bias correction adjusted GCM model over or underprediction of observed climate and caused the various GCM 20th century predicted climates to become more similar. Climate anomalies were calculated for the GCM data by comparing their values to a mean baseline period, 1961–1990. These anomalies were then added (a ratios approach was used to correct the bias in precipitation data) to the mean CRU climatology (for the period 1961–1990) to create a 1901–2100 monthly time series. The number of wet days per month, required for distributing monthly precipitation to daily amounts (Gerten *et al*., 2004), were not available from the GCMs. For this input, we repeated the 1960–1991 monthly wet days throughout the 21st century and assumed that changes in total monthly precipitation were more influential on modeled processes than the number of monthly wet days. Soil type corresponded to the FAO classification (Zobler, 1986). Atmospheric CO_2 data, as well as the climate projections, corresponded to the SRES A2 storyline (Nakicenovic, 2000) because current CO_2 emissions most closely follow this trajectory (Raupach *et al*., 2007).

For all LPJmL simulations (flux tower and basin-wide), a 1000 year spin-up was made using the first 30 years of climate data (1901–1930). The transient climate simulation was performed following this spin-up. A weather generator randomly allocated monthly precipitation to daily values and a fixed random seed was used so that daily precipitation was distributed consistently between parameter sets. This process, the spin-up and transient simulations, was repeated for each new parameter set.

Evaluation datasets

Flux tower data for net ecosystem exchange (NEE) and its derived component fluxes, ecosystem respiration (R_{eco}) and gross primary productivity (GPP), were obtained from the Brazil Flux Network (da Rocha *et al*., 2009). Because of the challenges associated with implementing eddy covariance in tropical sites, site-specific quality control procedures and gap-filling routines were implemented by LBA-MIP at the Biogeochemical Ecology Research Laboratory at the University of Arizona to produce a consistent monthly resolution time series. These algorithms used site-specific nighttime friction velocity (u^*) filters, various time averaging windows to estimate nighttime R_{eco}, and look-up tables [that included

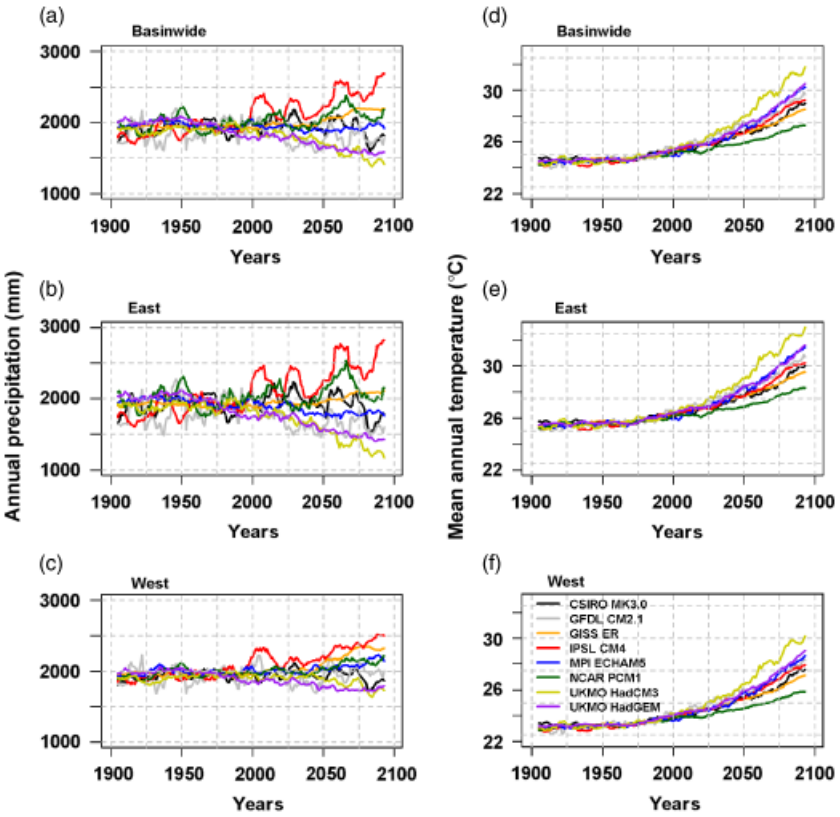

Fig. 2 Annual precipitation (a–c) and annual air temperature (d–f) projections of climate data used in LPJmL simulations (a 10-year moving average was applied to smooth interannual variability for presentation purposes).

photosynthetic active radiation (PAR)] to estimate missing GPP. Despite the uncertainty associated with gap-filling, the datasets provide spatially and temporally consistent data with which we could evaluate LPJmL fluxes.

Benchmarking

Benchmarking was used to eliminate extreme parameter set combinations resulting in unrealistic simulated ecosystem fluxes or stocks in comparison with observations. For example, some parameter sets contained values that had multiplicative effects on LPJmL processes, e.g., a set containing both very low light-use efficiency and slow sapwood turnover could produce abnormally low carbon stocks. To resolve this problem, carbon stocks and fluxes from field observations, generally known within at least $\pm 30\%$ (Saatchi *et al.*, 2007), were used to remove extreme LPJmL parameter sets.

This benchmarking approach was implemented twice using biomass data, first for the site level simulations, and then again at the basin level. For each site, aboveground biomass data were available from several field surveys (Baker *et al.*, 2004; Malhi *et al.*, 2006) and the mean and standard deviation of these calculated to compare with LPJmL-simulated carbon stocks. Parameter values causing extreme biomass outliers were identified (see parameters in parentheses in Table S1) and the parameter range adjusted before running the basin-wide simulations. For the basin-wide simulations, we used data for aboveground biomass from Saatchi *et al.* (2007) and Houghton *et al.* (2001) to remove unrealistic simulations before conducting the variance partitioning analysis ('Variance partitioning').

Estimating parameter importance

We used several techniques to explore the importance of the parameters on LPJmL processes. First, we evaluated output from the flux tower simulations to eliminate parameters that were not a significant source of uncertainty in LPJmL. We did this by estimating the ranked partial correlation coefficient (RPCC) for each parameter for a subset of LPJmL outputs (Zaehle *et al.*, 2005). The RPCC measures the significance of the relationship between parameter variability and model output, and was calculated with the 30-year mean (1971–2000) of the following variables; annual fluxes for GPP, net primary production (NPP), dry season NEE, R_{eco}, and evapotranspiration (ET) and for the state variables, vegetation and soil carbon content, tropical evergreen cover, and soil moisture content. An absolute cut-off RPCC value of <0.2 at any of the six flux sites was used in order to select the most important parameters for the basin-wide simulations (Zaehle *et al.*, 2005). To investigate the characteristics of which parameter set(s) best matched the measurements we also calculated a root mean

square error (RMSE) for observed NEE, R_{eco}, and GPP for each parameter set with the corresponding simulations.

For the analysis of the basin simulations, we used the same RPCC approach to explore spatio-temporal patterns of parameter importance. This was implemented in a two-fold approach; first, for each individual GCM, we summarized parameter contributions to changes in the main variables related to the Amazon 'dieback' hypothesis, carbon stocks and forest cover. Changes in vegetation and soil carbon, and tropical evergreen cover, were calculated between 1971–2000 and 2071–2098, for eastern and western Amazonia, the boundary defined by 65° west longitude following Malhi *et al*. (2009a). We then mapped (also for each individual GCM) the RPCC values for changes in these outputs at 1° spatial resolution.

Variance partitioning

We used a variance partitioning concept first presented in a simple climate model by Cox & Stephenson (2007) and implemented for GCMs by Hawkins & Sutton (2009). Using this approach, the importance of the various sources of uncertainty can be quantified for different regions at various timescales. A signal-to-noise ratio was then calculated to investigate the robustness of simulation output in the context of simulation uncertainty. The three sources of uncertainty considered were: (1) natural internal variability, the natural fluctuations of model responses to short-term climate variability (IV), (2) global climate model uncertainty (GCM), and (3) vegetation model uncertainty (LPJmL). These were estimated for both the eastern and western portion of the Amazon Basin (as defined previously) for LPJmL outputs directly related to Amazon dieback (vegetation and soil carbon, and tropical evergreen cover).

Before calculating the variance components, each individual LPJmL simulation (200 parameter sets × 8 GCMs) was referenced to its 1961–1990 mean to represent the change from this climatological period. A fourth order polynomial was fit to each time series from which the IV, LPJmL, and GCM components were calculated. The IV component is the variance of the residuals from each polynomial fit across all LPJml and GCM simulations. The LPJmL component was the mean of the variance of the polynomial fits for each GCM simulation. The GCM component was calculated as variance of the mean predictions for each individual climate model. Further details on this method can be found in Hawkins & Sutton (2009).

Results

Flux tower RPCC and RMSE

The most important parameters (RPCC > 0.4) contributing to the variability of yearly NEE (Table 4), soil and vegetation carbon stocks (Tables S2 and S3), and GPP (Table S4) at the flux sites were related to photosynthetic capacity (light-use efficiency and a photosynthetic parameter related to fraction of absorbed photosynthetic available radiation). At intermediate importance

Table 4 Ranked partial correlation coefficients for individual flux sites (fulfilling criteria of being of greater magnitude than an absolute value of 0.2 at any site)

Dry season net ecosystem exchange (NEE)							
	→ Wet climate to dry climate →						
Parameter name	Manaus KM34	Ji Parana	Santarem KM67	Santarem KM83	Bananal Island	Reserve Pe de Gigante	
Photosynthesis parameter adjusting PAR for canopy complexity (TrEV)	0.593	0.459	0.418	0.45	0.223	0.355	
Maximum evapotranspiration rate (mm day^{-1}, TrEV)	−0.5	−0.324	−0.463	−0.485	−0.374	−0.656	
Photosynthesis parameter adjusting PAR for canopy complexity (TrRG)	−0.458	−0.503	0.092	−0.057	−0.3	−0.296	
Intrinsic quantum efficiency of CO_2 uptake in C_3 plants	0.432	0.016	0.761	0.679	−0.1	0.129	
Sapwood turnover (years, TrEV)	0.333	0.194	0.177	0.17	0.132	0.148	
Sapwood turnover (years, TrRG)	−0.307	−0.287	−0.176	−0.2	−0.093	−0.134	
Maximum evapotranspiration rate (mm day^{-1}, TrRG)	0.214	0.236	0.085	0.165	0.202	0.442	
Leaf longevity threshold for raingreens (days)	−0.192	−0.322	−0.139	−0.305	−0.634	−0.469	
Albedo (unitless)	−0.152	−0.034	−0.257	−0.221	0	−0.057	
Rooting distribution (fraction, TrEV)	0.144	−0.028	0.295	0.168	0.084	−0.06	

The sites are ordered from left to right in terms of dry season length. A positive correlation indicates that variability in dry season NEE is positively correlated with changes in the parameter value. These parameters were selected for the full basin-wide simulation parameter set.
PAR, photosynthetic active radiation.

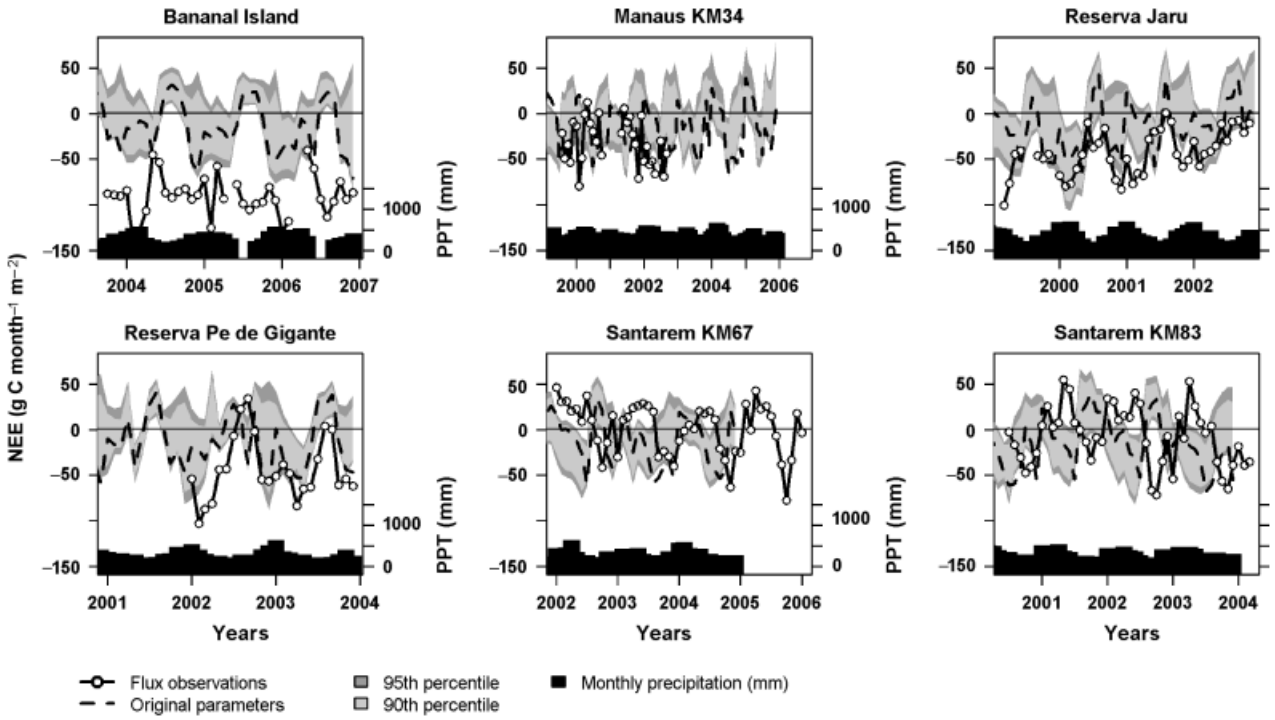

Fig. 3 Net ecosystem exchange (NEE) for the six flux tower sites [NEE = NPP−RH (heterotrophic respiration)]. Confidence intervals are generated from the 1000 parameter set combinations and following simulations. NPP, net primary production.

(RPCC = 0.3–0.4) were parameters determining carbon allocation and vegetation dynamics (i.e., sapwood turnover and maximum establishment rate). Also important at the wet sites (RPCC = 0.2–0.3), but higher at the dry sites, were parameters related to water use (rooting distribution and maximum ET). Temperature-related parameters, such as those used to determine photosynthetic enzyme stress or tissue and growth respiration, were not significantly correlated with variability in carbon or water fluxes.

Compared with observations, the magnitude of simulated carbon fluxes were within the range of measured NEE (Fig. 3). However, the monthly modeled fluxes were generally out of phase with observations reflecting a combination of possible problems in model parameterization, measurement error and unique local-site conditions. For example, the RMSE was highest at the Bananal Island site ($85.8\,g\,C\,m^{-2}\,month^{-1}$ for NEE) where a 4–5 month inundation period (Borma *et al.*, 2009) reduces soil respiration fluxes (Fig. S2) – a process not modeled with LPJmL. However, measurement error at Bananal Island may also be high because of the flooded soil conditions and possible dissolved organic carbon losses not measured with the eddy covariance technique. At drier sites, the RMSE was lower (38.7–$40.5\,g\,C\,m^{-2}\,month^{-1}$) because of a more distinct seasonal precipitation cycle that clearly limited GPP and soil respiration in the dry season (Figs S1 and S2). At the wetter, terra firme sites (KM34, KM67, and KM83), NEE RMSE ranged between 25.4 and $48.5\,g\,C\,m^{-2}\,month^{-1}$ with seasonal out-of-phase problems associated with dry-season declines in simulated GPP, whereas observations suggest sustained dry-season GPP.

For soils and rooting depths, the parameter sets corresponding to the lowest RMSE for NEE and GPP were generally consistent with field observations suggesting deep soil and rooting depths (Table 5). Deeper soil and root profiles were more important at the wetter sites in order to offset dry-season moisture limitations on photosynthesis, whereas at the dry sites, water limitation occurred in the dry season regardless of soil depth. The maximum ET rate parameter, which determines simulated evaporative supply, had lower error with higher parameter values for the wet sites than for the drier sites in order to continually provide moisture for maintaining stomatal conductance. For both wet and dry sites, error was lowest with albedo reduced to 0.12, from the global mean default value of 0.17, resulting in more efficient use of PAR and photosynthesis rates.

We found that compared with observed carbon stocks, the LPJmL simulations tended to underestimate standing biomass (Fig. 4). Using the benchmarking approach, we removed parameter set simulations where modeled biomass was outside of a $\pm$ 30%

Table 5 Mean value and range, for selected parameters that were in the lowest root mean square error (RMSE) category

Parameter name (with units)	Wettest site (Manaus KM34)		Driest site (Pe de Gigante)	
	GPP	NEE	GPP	NEE
Lower soil depth (cm)	5983.8 (1806.9–9927.3)	5992.5 (2318.5–9366.3)	3789.8 (1099.6–9123.8)	4316.2 (1000–7538.6)
Maximum evapotranspiration rate (mm day^{-1}, TrEV)	6.2 (5.4–6.8)	5.8 (4.7–6.6)	4.7 (3.8–6.4)	5.9 (5.1–7.0)
Rooting distribution (fraction, TrRG)	0.76 (0.63–0.83)	0.80 (0.60–0.99)	0.83 (0.65–0.97)	0.84 (0.60–0.98)
Rooting distribution (fraction, TrEV)	0.72 (0.61–0.88)	0.84 (0.64–0.99)	0.72 (0.60–0.96)	0.69 (0.62–0.85)
Albedo (unitless)	0.12 (0.08–0.14)	0.12 (0.11–0.16)	0.12 (0.08–0.15)	0.12 (0.09–0.17)

GPP, gross primary production; NEE, net ecosystem exchange.

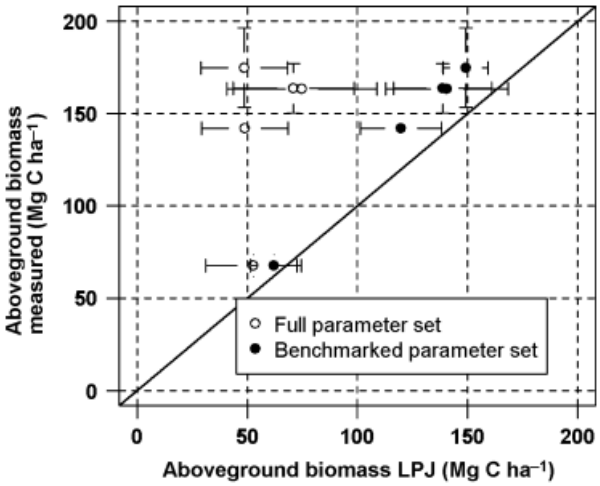

Fig. 4 Correlation between observed and simulated aboveground biomass. Standard error from simulated is calculated from the 1000 parameter sets. For the observed, if multiple studies available, a standard error was computed. The benchmarked data points represent simulations that were within 30% of the observed mean values.

margin of error around the observed values. We identified four parameters contributing erroneously low biomass values; these were related to slow sapwood and leaf turnover rates, and low light-use efficiencies (quantum-use efficiency and extinction coefficient) used in photosynthesis (Table 1). Slow sapwood turnover and low light-use efficiency results in large diameter, slow-growing trees, and underestimates of aboveground live biomass. The range of each of these parameters was adjusted to be more similar to the original value used in Sitch *et al*. (2003) and these revised parameters used in the basin-wide simulations. Of the total set of 41 parameters, we subset 21 parameters that had an absolute RPCC value >0.2 to be included in the basin-wide simulations (Table 2).

Basin-wide RPCC for changes in carbon and vegetation

The subset of 21 parameters (using the revised parameter ranges for four of the parameters) was used to generate 200 basin-wide simulations for each of eight GCM projections. The average basin-wide simulations reproduced carbon stocks within the range of previous field and remote sensing studies for the averaging period of 1971–2000. However, there remained the tendency for the carbon stock estimates to be on the low-end of corresponding observations (Table 6). For example, across all 1600 simulations, 20th century aboveground carbon stocks averaged 48.7 Pg C (and ranged between 11.6 and 175.8 Pg C) compared with estimates of 59–73 Pg C for aboveground live biomass by Saatchi *et al*. (2007) and 33–93 Pg C from Houghton *et al*. (2001). Soil carbon estimates were similar to previous studies and ranged from 34 to 36 Pg C compared with 33–39 Pg C (Bernoux *et al*., 2002). For the benchmarking of the basin-wide simulations, we removed parameter sets which resulted in regional carbon estimates outside the range of observed aboveground live biomass (55–110 Pg C). About 25% of the simulations passed this test (the removed simulations generally included slow turnover rates and low light-use efficiency parameters), and were used for the variance partitioning modeling ('Fractional and absolute variance, and signal-to-noise ratios').

Basin-wide responses to climate change for tree cover (Fig. 5a), aboveground live biomass (Fig. 5b) and soil carbon (Fig. 5c) varied significantly between climate scenarios but little among parameter sets. The long-term changes in tree cover, and above- and below-ground carbon stocks also varied in spatial pattern and magnitude among climate projections. In Western Amazonia there was a slight decrease to no change in tropical evergreen cover for the CSIRO, GISS, and MPI GCMs, whereas in Eastern Amazonia, three GCMs

Table 6 Average Amazon Basin (1971–2000) summary of tree cover and carbon stocks compared with observations from eight GCMs

LPJmL variable	Range (+ standard deviation)	With benchmarking [using Saatchi *et al.*'s (2007) biomass estimate]	Observations
Tropical evergreen cover (%)	58.79 (13.96)	61.16 (16.66)	None
Aboveground C-storage (Pg C)	48.79 (16.76)	67.28 (11.44)	39–93 Pg C (Houghton *et al.*, 2001) 69–103 Pg C (Saatchi *et al.*, 2007)
Belowground C-storage (Pg C)	35.13 (7.51)	30.69 (5.91)	33–39.8 Pg C (Bernoux *et al.*, 2002)

On average, 25% of the parameter sets met the benchmarking criteria and were used in the variance partitioning model.
GCMs, general circulation models.

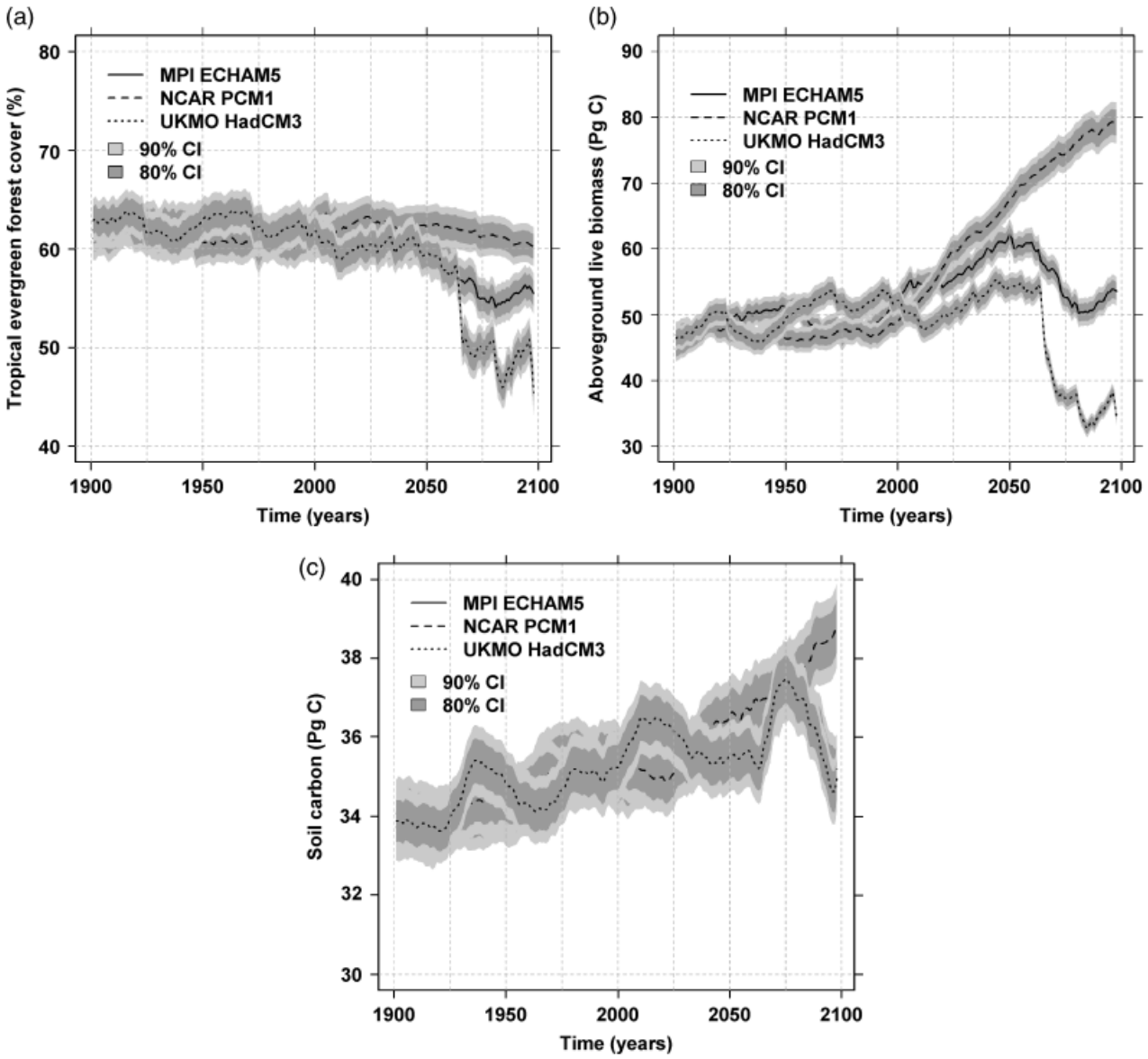

Fig. 5 Changes in ecosystem variables for three different climate projects representing changes to a wet, stable, and dry precipitation regime (Fig. 2) for (a) tropical evergreen forest cover (b) aboveground live biomass, and (c) soil carbon stocks.

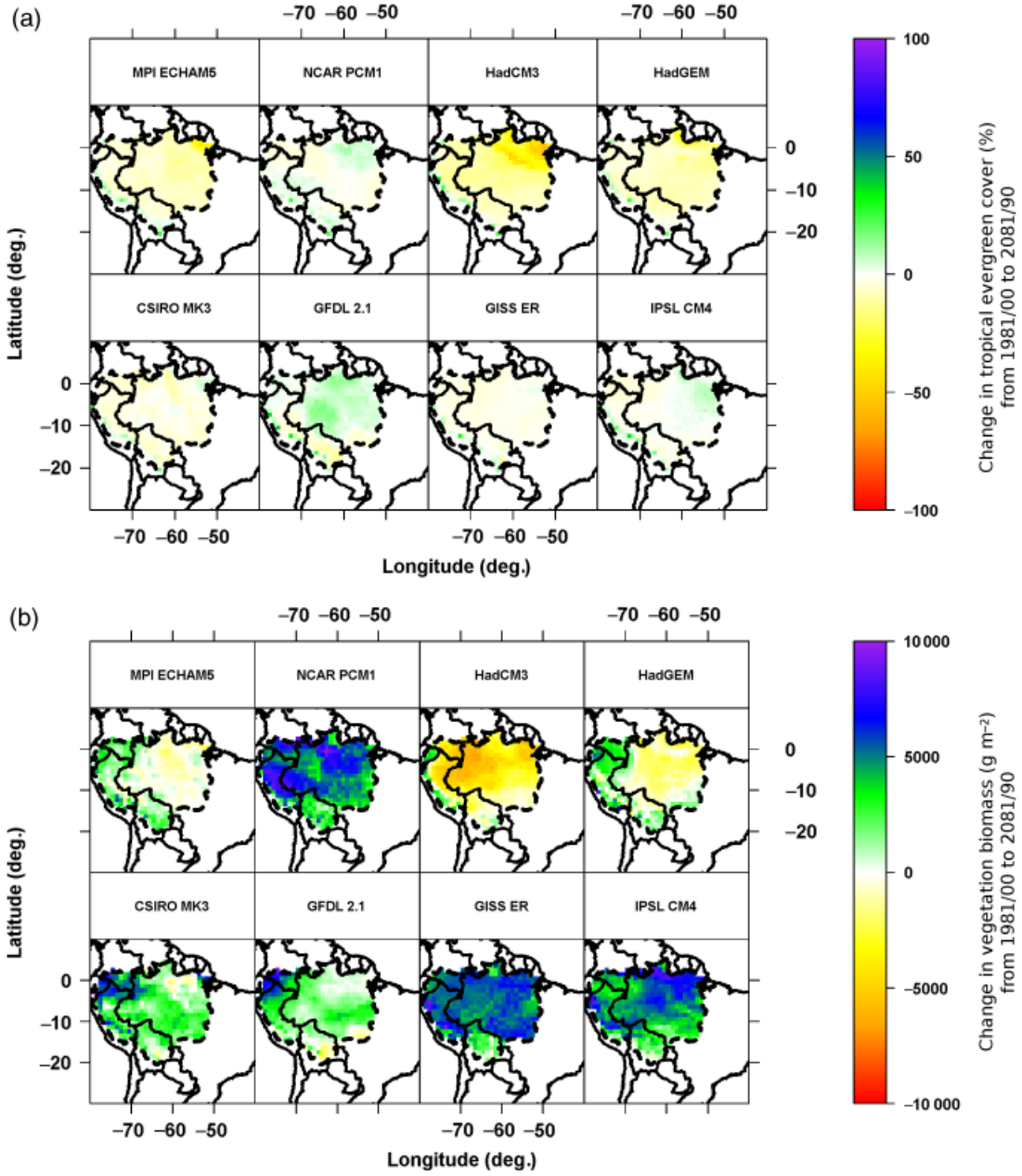

Fig. 6 (a) Change in vegetation carbon for all general circulation models (GCMs), (b) change in tropical evergreen cover (changes in soil carbon in Supporting Information). Dashed line represents the hydrologic delineation of the Amazon Basin.

projected increases in tropical evergreen cover and three other GCMs projected decreases (Fig. 6a). Changes in vegetation carbon were equally variable between models and within the basin (Fig. 6b). Both HadCM3 and HadGEM projected large decreases in carbon stocks compared with the NCAR, GISS, and IPSL that projected increases (Fig. 6b). MPI, CSIRO and GFDL projections resulted in little to no change in vegetation carbon. Changes in soil carbon stocks were more consistent, with little to small increases occurring (Fig. S3).

The Hadley CM3 climate projection was associated with the most extreme climatic drying and warming scenario (Fig. 2) and resulted in the largest vegetation carbon losses (Fig. 6b). For this scenario, the most important parameters (Table 7) determining the magnitude of changes in carbon stocks were related to vegetation dynamics and water use. For all climate scenarios,

Table 7 Ranked partial correlation coefficients for changes in vegetation carbon (1981/2000 to 2081/2098) for the Eastern and Western Amazon Basin

	CSIRO MK 3.0		GFDL CM 2.1		GISS E-R		IPSL CM4		MPI ECHAM 5		NCAR PCM 1		UKMO HadCM3		UKMO HadGEM	
Parameter	East	West	East	West	East	West	East	West	East	West	East	West	East	West	East	West
Lower soil depth	0.22	0.09	−0.01	0.15	*−0.02*	*0.02*	*0.14*	*−0.12*	0.17	*−0.01*	*0.31*	*−0.06*	−0.25	0.03	−0.13	0.05
Max. evapotranspiration rate (TrRG)	−0.03	−0.06	0.07	−0.06	*−0.08*	*−0.01*	*−0.03*	*−0.01*	0.10	*0.06*	*−0.07*	*−0.09*	0.17	0.20	0.19	−0.02
Max. evapotranspiration rate (TrEV)	0.20	0.25	−0.11	0.13	*0.10*	*−0.01*	*0.14*	*−0.09*	−0.09	*0.09*	*0.29*	*0.14*	−0.52	−0.08	−0.36	0.20
Maximum establishment rate	−0.64	−0.80	−0.25	−0.52	*−0.71*	*−0.64*	*−0.81*	*−0.77*	0.31	*−0.44*	*−0.85*	*−0.78*	0.59	0.27	−0.39	−0.61
Rooting distribution (TrRG)	0.03	0.07	−0.22	−0.27	*0.15*	*0.07*	*0.08*	*0.09*	−0.15	*−0.06*	*0.23*	*0.11*	−0.04	−0.01	−0.18	0.02
Rooting distribution (TrEV)	−0.66	−0.54	−0.13	−0.41	*−0.30*	*−0.02*	*−0.56*	*−0.09*	−0.38	*−0.42*	*−0.69*	*−0.26*	0.63	0.11	0.52	−0.34
Leaf longevity threshold for raingreens	0.12	−0.09	−0.05	−0.08	*0.18*	*0.03*	*−0.07*	*0.01*	0.21	*−0.11*	*−0.15*	*−0.06*	0.15	0.05	−0.04	0.04
Leaf to root biomass ratio under non−water stressed conditions (TrRG)	0.19	0.01	0.14	0.05	*−0.09*	*−0.06*	*−0.03*	*−0.01*	0.12	*−0.03*	*−0.09*	*−0.14*	0.22	0.09	0.04	−0.07
Albedo	−0.03	0.03	−0.03	0.03	*−0.11*	*−0.01*	*−0.09*	*−0.04*	−0.14	*−0.09*	*−0.04*	*−0.12*	−0.05	0.05	0.02	0.11
Leaf respiration as a fraction of Rubisco capacity in C_3 plants	0.05	0.09	−0.04	−0.03	*0.13*	*0.01*	*0.15*	*0.18*	−0.05	*0.11*	*0.26*	*0.28*	0.07	−0.02	0.22	0.07
Sapwood turnover (TrRG)	−0.23	0.01	−0.53	−0.34	*0.02*	*−0.08*	*0.02*	*0.03*	−0.34	*0.03*	*0.05*	*−0.06*	−0.04	0.05	0.08	−0.08
Sapwood turnover (TrEV)	−0.25	−0.39	−0.38	−0.23	*−0.29*	*−0.25*	*−0.46*	*−0.39*	0.02	*0.00*	*−0.26*	*−0.46*	0.64	0.60	0.64	−0.03
Leaf turnover (TrEV)	−0.02	0.06	−0.03	−0.02	*−0.07*	*−0.03*	*−0.02*	*0.02*	−0.07	*0.13*	*−0.03*	*0.07*	−0.01	0.08	−0.06	−0.03
Intrinsic quantum efficiency of CO_2 uptake in C_3 plants	0.30	0.45	0.29	0.47	*0.51*	*0.55*	*0.37*	*0.40*	0.36	*0.32*	*0.28*	*0.60*	−0.08	−0.21	−0.42	0.26
Intrinsic quantum efficiency of CO_2 uptake in C_4 plants	−0.01	0.14	0.05	0.07	*0.04*	*0.08*	*0.12*	*0.13*	−0.11	*0.04*	*0.03*	*0.09*	−0.05	−0.12	−0.10	0.08
Photosynthesis scalar param. (TrRG)	0.25	−0.24	0.12	0.16	*−0.12*	*−0.19*	*−0.13*	*−0.21*	0.43	*−0.28*	*−0.24*	*−0.21*	0.48	0.00	0.02	−0.18
Photosynthesis scalar param. (TrEV)	0.09	0.61	0.18	0.49	*0.67*	*0.62*	*0.58*	*0.58*	−0.18	*0.32*	*0.56*	*0.71*	−0.66	−0.50	−0.55	0.23
Photosynthesis co-limitation parameter (θ)	−0.14	−0.07	0.13	0.18	*−0.13*	*−0.09*	*−0.13*	*−0.20*	0.01	*−0.13*	*−0.20*	*−0.07*	−0.23	−0.25	−0.53	−0.21
Light extinction coefficient	0.00	−0.03	0.09	0.06	*0.05*	*0.07*	*−0.13*	*−0.15*	0.10	*0.03*	*−0.12*	*−0.07*	0.06	0.19	0.04	0.13
Specific leaf area (TrRG)	0.12	−0.01	0.06	−0.01	*0.06*	*0.03*	*0.05*	*0.05*	0.11	*−0.02*	*0.08*	*0.06*	0.10	0.05	0.01	0.04
Specific leaf area (TrEV)	−0.08	−0.23	−0.13	−0.13	*−0.18*	*−0.16*	*−0.19*	*−0.14*	0.11	*−0.10*	*−0.15*	*−0.19*	0.23	0.25	0.27	−0.15

The RPCC values must be interpreted in the context of the directly change of vegetation carbon for each model, these are illustrated in Fig. 7. The RPCC columns in italics highlight the GCMs which project a wetter climate by 2100.

RPCC, ranked partial correlation coefficient; GCMs, general circulation models.

 Global Change Biology, doi: 10.1111/j.1365-2486.2009.02157.x

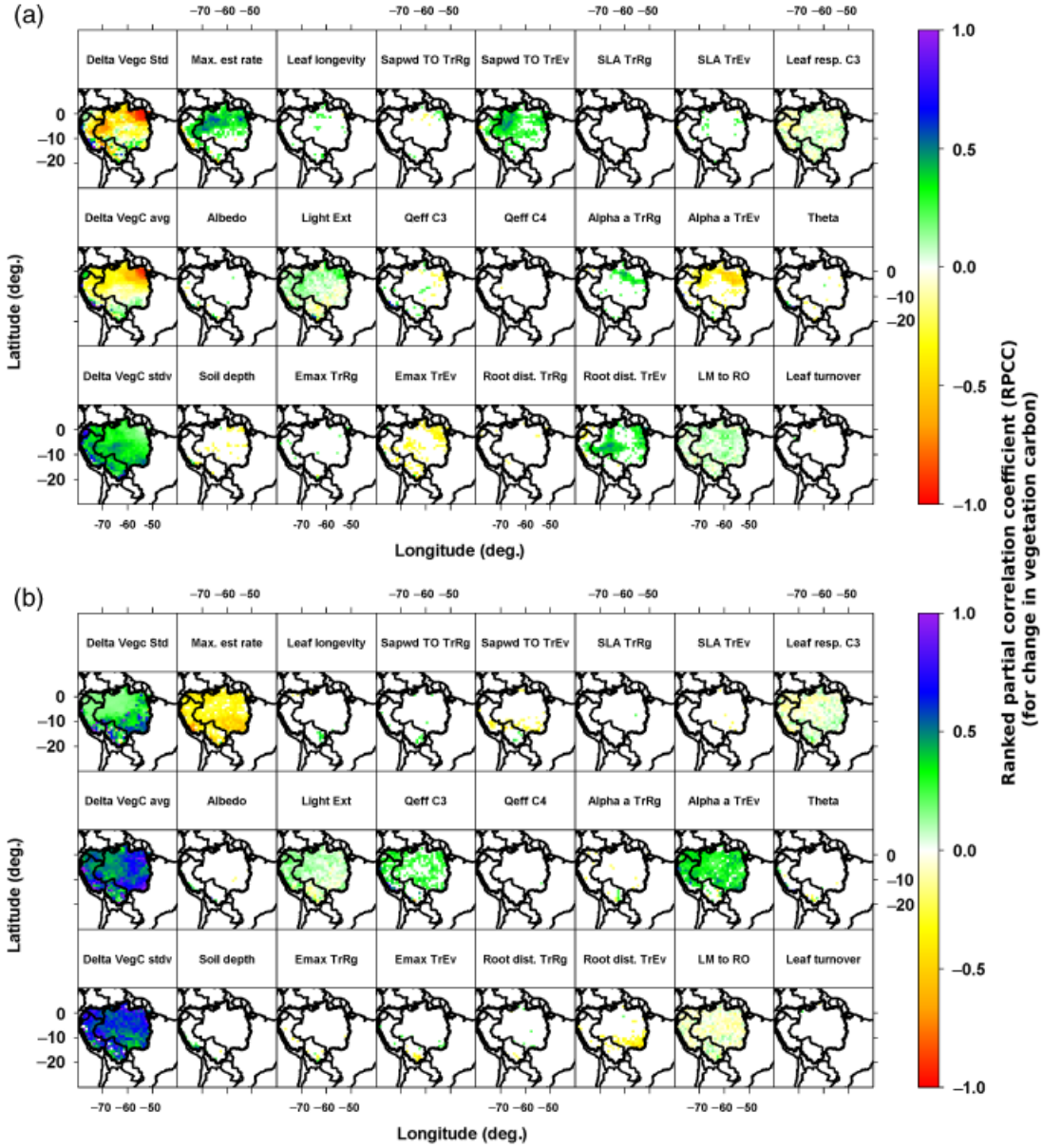

Fig. 7 Ranked partial correlation coefficient (RPCC) spatial patterns for changes in vegetation carbon (1991–2000 vs. 2090–2098) for all 21 parameters (see Table 1 for references) used for the basin-wide Latin hypercube analysis for the HadCM3 climate projection. The change in vegetation carbon for the standard parameter set, mean change in vegetation carbon for all parameter sets, and standard deviation for all parameter sets is also shown. The first row corresponds to parameters related to carbon allocation, the second row for photosynthesis, and the third row contains parameters related to water use. The RPCC correlations are shown for the Hadley CM3 (a), which projects a drier climate and GISS ER (b), which projects a wetter climate and increases in aboveground live biomass.

high maximum establishment rate reduced the amount of aboveground carbon due to competition among individuals. This was because the establishment rate determines tree density and corresponding competition for light and water. Under a drier climate, high establishment rates allow for rapid recolonization following mortality (from drought or fire) decreasing the relative change in carbon losses. Under wetter future climates, a high maximum establishment rate caused competition to increase, causing changes in biomass to be reduced. In terms of water use, a higher proportion of roots in the upper soil layer appeared to be a disadvantage under a drying climate because of less access to deep water storage (resulting in a negative correlation between rooting distribution and changes in aboveground live biomass, bottom row, Fig. 7a). Under wet climate

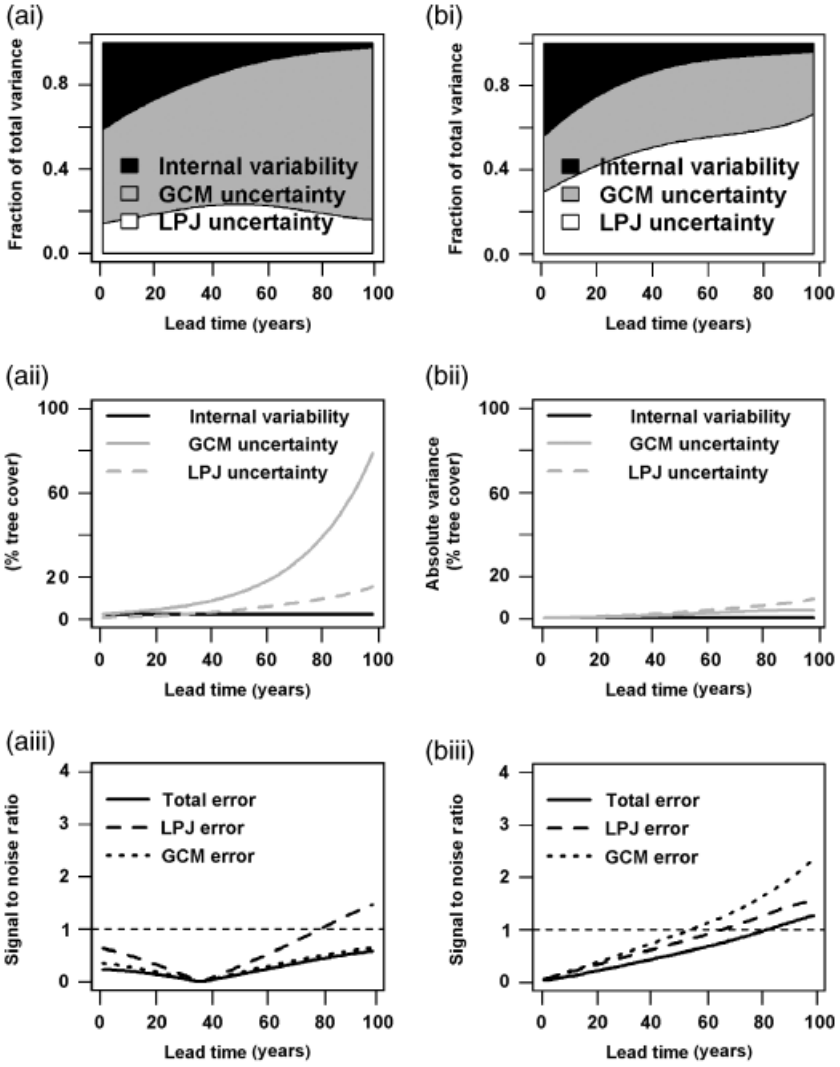

Fig. 8 Summary of variance partitioning for tropical evergreen tree cover. The lead time is the number of years since year 2000. Figures (ai, aii, and aiii) are for the Eastern Amazon and (bi, bii, and biii) for the Western Amazon.

projections, however, water-related parameters (bottom row of Fig. 7b) became relatively less important and limitations related to photosynthesis (e.g., light extinction coefficient, light-use efficiency) become more important on the changes in carbon storage.

Changes in soil carbon stocks were strongly coupled to aboveground processes regulating productivity and rates of litterfall (Fig. S4). Under the dry climate projections, soil carbon losses increased with parameter combinations that increased aboveground productivity i.e., the photosynthesis scaling parameter and quantum use efficiency (Table S6). Soil carbon losses decreased with parameters that reduced litter inputs through mortality, most notably increased deep rooting and decreased maximum ET. Under wetter climates, soil carbon stocks increased because of increased aboveground productivity and litterfall inputs, the parameters limiting productivity were all positively correlated with soil carbon (Table S6).

Changes in tropical broadleaf evergreen tree cover exhibited similar directional changes as vegetation carbon stocks although less spatial variability (Fig. 6). The response of tropical evergreen vegetation cover to climate was dependent not only on parameter values, but also to competition with the drought deciduous PFT. For example, high light-use efficiency of the tropical drought deciduous PFT resulted in large decreases in tropical evergreen cover. In the short-term, it was competitively advantageous for the tropical evergreen PFT to have high leaf longevity and deeper rooting profiles, but these traits also made the PFT more resilient to climatic stress. For the wetter climates, indirect controls on productivity (maximum ET rate, root distribution,

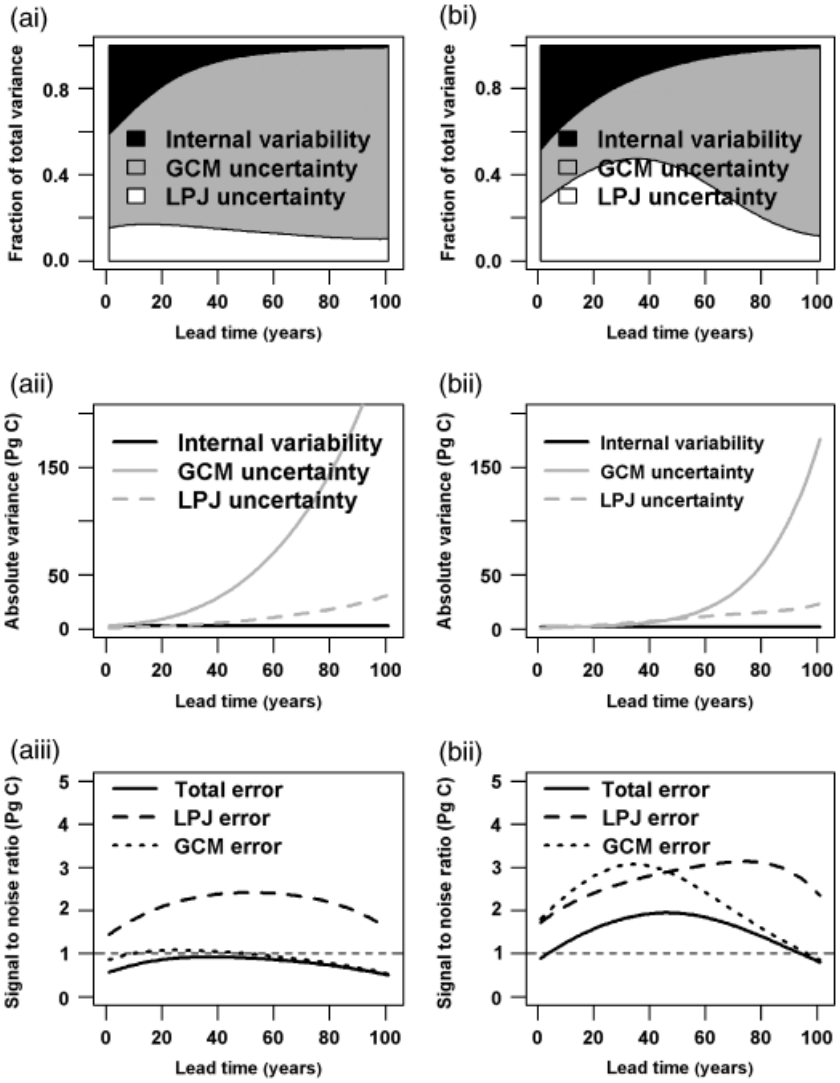

Fig. 9 Summary of variance partitioning for vegetation carbon. The lead time can be thought of as year 2000 equal to lead time 0. Figures (ai, aii, and aiii) are for the Eastern Amazon and (bi, bii, and biii) for the Western Amazon.

and leaf-mass to root-ratio) were increasingly important, presumably because competition with the tropical drought deciduous PFT became more of a limiting factor than climate.

Fractional and absolute variance, and signal-to-noise ratios

The benchmarked basin simulations ('Basin-wide RPCC for changes in carbon and vegetation') were used to partition variance between the IV, LPJmL, and GCM components. This approach was used to better understand the spatio-temporal dynamics and robustness of the various sources of uncertainty of the model output variables. These are illustrated as their relative fractions and absolute values for tropical evergreen cover (Fig. 8) and vegetation carbon (Fig. 9) for East and West Amazonia. The lead time dependence of variance partitioning varies between LPJml outputs, and is dependent on the geographic area of interest.

Averaged across all GCM scenarios, the decrease in evergreen tree cover is small ($<$1.5% by 2050 and $<$4.5% by 2100) and the variations between climate projections large, resulting in low signal-to-noise ratios (Fig. 8). In Eastern Amazonia, a large portion of the total uncertainty is from the GCM component. However in Western Amazonia, both LPJmL and GCM uncertainty contribute approximately equal variance as the GCMs are more consistent in their projected climate regimes, at least through the mid-21st century (Fig. 2).

The sources of variability in changes in aboveground biomass are, in general, similar to tree cover dynamics. By 2050, basin-wide changes in vegetation carbon stocks increased from 3.3 to 12.7 Pg C, but by 2098, this change in carbon stocks diverged to between a −16.4 Pg C decrease and a 19.1 Pg C increase. In Eastern Amazonia, the signal-to-noise ratio (mean change in output variable divided by square root of the total variance) was lower than in the West, reflecting the large variability in climate projections that led to either increased or decreased vegetation carbon stocks (Fig. 6). In Western Amazonia, there was more agreement across GCM climate projections and the signal-to-noise ratio suggests that up to 2050–2060, changes in vegetation carbon are relatively robust. Post-2050, variability in GCM projections decreases the signal-to-noise ratio and in 2080, this becomes <1.

Discussion and conclusions

State of DGVM understanding of tropical processes

Our analysis of parameter uncertainty and its effects on carbon stocks and fluxes illustrates that there remains large uncertainty for modeling tropical processes under changing climates. With the present-day climate, the agreement between seasonal LPJmL simulations and observations of carbon fluxes is relatively poor, suggesting that processes, in addition to parameters, remain inadequately characterized. In addition to hydrologic and light-use-related processes, the seasonal release of nutrients (i.e., phosphorous) can also exert some control on dry to wet season differences in GPP (Grant *et al*., 2009). Within LPJmL, much of the uncertainty appears to come from a relatively small subset of model parameters that are related to light-dependent photosynthetic processes (for the fluxes) and vegetation dynamics (for stocks). To reduce parameter uncertainty, future field research must provide statistically representative samples of structural and physiological measurements to assist in parameter optimization. In addition, site-specific characteristics (i.e., the presence of seasonally flooded soils) and observational error may also contribute to the low correlation between observations and simulations. Our site-level results are similar to previous analyses conducted for global (Zaehle *et al*., 2005) and northern-temperate regions (Wramneby *et al*., 2008), suggesting that parameter sensitivities and their importance are similar across multiple biomes.

Under climate change, we find that changes in vegetation and soil carbon pools are determined mainly by parameters related to vegetation dynamics (i.e., maximum establishment rate) and competition (i.e., rooting depths). Parameters related to photosynthesis (e.g., light-use efficiency) are important in determining the initial carbon stocks, but more importantly, those parameters related to vegetation dynamics determine the pace of ecosystem recovery, or biome change, following drought or fire-related forest mortality. The simulated interactions between fuel accumulation and fire frequency concur with other studies that suggest shifts in Amazonian forest composition to savanna systems will likely be mediated by changes in disturbance regime (Malhi *et al*., 2009a). The different parameter sets did not influence the trajectory of ecosystem response to climate (Fig. 5a–c), for example, under the drier climate projections, LPJmL projected carbon losses and decreases in tropical evergreen cover regardless of parameter combination (see mean and standard deviation of responses in Fig. 7a and b).

The apparent lack of importance of temperature-dependent processes (i.e., growth and maintenance respiration, or those parameters related to photosynthetic biochemistry) may be due to several reasons. First, the photosynthesis scheme in LPJmL uses the Haxeltine & Prentice (1996b) derivation for calculating canopy maintenance respiration. With this approach, canopy respiration is directly related to the maximum carboxylation rate of photosynthesis (V_{cmax}), an indicator of leaf nitrogen content, which is shown to be positively correlated with leaf respiration in tropical forests (Cavaleri *et al*., 2008). This formulation decreases the temperature dependence of NPP to canopy respiration, which can account for the majority of autotrophic respiration fluxes (Malhi *et al*., 2009b). The rates of sapwood and root respiration follow the Lloyd & Taylor (1994) approach that is related to Q_{10} factor (the change in respiration rate with a 10 °C change in temperature), but because they constitute a smaller contribution to autotrophic respiration, their temperature-dependent parameters are less important in full ecosystem scale assessment. Simulated soil respiration is already close to its maximum in tropical ecosystems, and so there is little potential for increased soil respiration or a large sensitivity to climate change.

This analysis of the relative importance of the parameters determining the scale of 'dieback' highlights the significance of including vegetation dynamics when considering ecosystem responses to climate. Equilibrium models that do not include vegetation dynamics, i.e., Salazar *et al*. (2007), may over- or underestimate ecosystem response to climate impacts if the process of vegetation recovery or competition is excluded. We found that with higher establishment rates there was faster recovery of aboveground live biomass following disturbance. This led to a lower rate of change in forest cover or carbon stocks for LPJmL, but did not alter the overall trajectory of ecosystem response to climate change.

GCM variability

The variance partitioning approach attributed much of the long-range uncertainty of Amazon dieback to divergence in late-21st century climate projections. However, this contribution may be somewhat reduced if uncertainty related to DGVM structure is also considered (i.e., by comparing multiple DGVMs to one another in a model-intercomparison framework). While we investigated only multiple-versions of the same DGVM structure, intermodel comparison projects have shown Amazon dieback to be ubiquitous across multiple DGVMs, with the main difference between models in the extent and magnitude of dieback (Cramer *et al*., 2001; Cox *et al*., 2004; Sitch *et al*., 2008). Different DGVM structures may result in higher or lower temperature responses of the carbon cycle (Galbraith D, Huntingford C, Cox PM, Levy PE, Sitch S, Meir P, Williams M, unpublished results) or models may ignore CO_2 feedbacks on water-use efficiency (Salazar *et al*., 2007) that may ameliorate dieback to a certain extent (Lapola *et al*., 2009; Poulter *et al*., In press). Coupled carbon-climate models also include important positive feedbacks on climate that offline models ignore, for example at the regional scale, approximately 20% of Amazon drying occurred from reductions in transpiration (Betts *et al*., 2004). Despite the uncertainty related to the representation of processes, the multiple GCM projections and their magnitude of combined drying and warming over the Amazon Basin appear to contribute the largest source of uncertainty for forest dieback.

The results here present a challenge for assessing the strength of future global carbon cycle feedbacks and for implementing adaptation and mitigation strategies to maintain ecosystem services. The uncertainty in Amazon climate projections has been acknowledged in several previous studies (Li *et al*., 2006; Malhi *et al*., 2008). Several shortcomings related to 20th century climate modeling of Amazon precipitation, are outlined by Malhi *et al*. (2009a) who present a combination of hypotheses ranging from the application of coarse-grid scales that do not capture fine-scale meteorological processes to the role of topography in determining the southern extent of the 'South American monsoon,' which most models overestimate. Much of the variability in future precipitation (-15% to $+10\%$) is related to changes in the parameterization of ocean dynamics among models (Li *et al*., 2006). Currently, the GCM that best captures 20th century climate patterns and realistically models the relationship between tropical climate and sea surface temperatures is the Hadley CM3 model, which also projects the greatest drying for the Amazon in the 21st century (Cox *et al*., 2008).

In Figs 8 and 9, the spatio-temporal effects of GCM uncertainty are presented. The GCM variance could be considered an underestimate because we focused on only one future emissions storyline and on those GCMs that met criteria for representing 20th century Amazon climate (Li *et al*., 2008; Reichler & Kim, 2008). Emissions uncertainty is independent from GCM uncertainty, with its contribution increasing during the 21st century and related to socio-economic development (Hawkins & Sutton, 2009). In the absence of GCM uncertainty, the signal-to-noise ratios for changes in carbon storage were robust throughout most of the 21st century (i.e. >1) and despite the contribution of uncertainty from LPJmL, adaptation and mitigation might follow robust findings that to assist policy making and decision process. The GCM variability reduces the signal-to-noise ratio below 1 for Eastern Amazonia for the entire 21st century and so further filtering of GCMs or improvements in the consistency of their projections is required before planning can be implemented with confidence. The changes in tree cover are generally of smaller magnitude than changes in vegetation carbon and the signal-to-noise ratio was remained small both spatially and with changing lead time. This suggests that more conspicuous indicators of ecosystem vulnerability to climate, such as carbon stocks, may be more useful for assessing climate impacts.

What is probability of Amazon dieback

While there remains strong disagreement between GCMs on the direction of precipitation changes across the Amazon Basin (IPCC, 2007), our study is consistent with previous research that shows there remains high risk of biome shifts in the Amazon under certain climate regimes (Scholze *et al*., 2006; Sitch *et al*., 2008). It is becoming clearer the probability of Amazon dieback for a given CO_2 rise scenario is highly dependent on GCM projections rather than dependent on ecosystem processes or their parameterization (Sitch *et al*., 2008). We found that the different parameter combinations did influence the timing and magnitude of carbon losses or vegetation shifts, but not the general trajectory of these responses. This was illustrated for scenarios which had deeper soil profiles or changes to the rooting distribution where neither change resulted in increased resilience of the Amazon or prevented dieback if the drying was significant. These findings have recently been supported by tropical field experiments, which have shown that after 1–2 years of precipitation reductions tree and liana mortality increase and productivity decreases (Nepstad *et al*., 2007; Brando *et al*., 2008). Other modeling studies using LPJmL have also shown that threshold responses for changes in aboveground live biomass may exist and are mostly related to decreases in precipitation (Cowling & Shin, 2006; Galbraith D,

Huntingford C, Cox PM, Levy PE, Sitch S, Meir P, Williams M, unpublished results).

Applications to impact analysis, mitigation, and adaptation

The method that we present for partitioning vegetation model uncertainty from GCM projection variability was developed to inform policy responses to climate change (Cox & Stephenson, 2007; Hawkins & Sutton, 2009). In the short-term (decadal scale), the contribution of model internal variability (from year to year climate fluctuations) decreases as the signal from climate change becomes stronger. Our results suggest that the optimal planning horizon, when signal-to-noise ratio is greatest, is spatially and temporally dependent. Over the short to medium term (10–60 years) the signal-to-noise ratio for changes in carbon stocks is highest, and investments over this time period would be associated with higher confidence. For changes in forest cover, the signal-to-noise ratio is less robust, suggesting that planning might focus on other indicators for ecosystem vulnerability.

Acknowledgements

We acknowledge funding from the Marie Curie Research Training Network 'Greencycles' (MRTN-CT-2004-512464), and helpful discussions with Ben Booth, David Galbraith, Phil Harris, Andrew Friend, and Chris Huntingford. We thank Scott Saleska and Gustavo de Goncalves for coordinating the LBA-Model Intercomparison Project that provided gap-filled eddy covariance data, and Wenhong Li for providing further information on GCM performance. The comments from anonymous reviewers greatly improved the discussion on DGVM uncertainty. We acknowledge the modeling groups, the Program for Climate Model Diagnosis and Intercomparison (PCMDI) and the WCRP's Working Group on Coupled Modelling (WGCM) for their roles in making available the WCRP CMIP3 multi-model dataset. Support of this dataset is provided by the Office of Science, U.S. Department of Energy.

References

Alton P, Mercado L, North P (2007) A sensitivity analysis of the land-surface scheme JULES conducted for three forest biomes: biophysical parameters, model processes, and meteorological driving data. *Global Biogeochemical Cycles*, **20**, GB1008, doi: 10.1029/2005GB002653.

Baker TR, Phillips OL, Malhi Y *et al*. (2004) Variation in wood density determines spatial patterns in Amazonian forest biomass. *Global Change Biology*, **10**, 545–562.

Bartelink HH (1998) A model of dry matter partitioning in trees. *Tree Physiology*, **18**, 91–101.

Bernoux M, Carvalho MCS, Volkoff B, Cerri CC (2002) Brazil's soil carbon stocks. *Soil Science Society of America*, **66**, 888–896.

Betts RA, Cox PM, Collins M, Harris PP, Huntingford C, Jones CD (2004) The role of ecosystem–atmosphere interactions in simulated Amazonian precipitation decrease and forest dieback under global warming. *Theoretical and Applied Climatology*, **78**, 157–175.

Bonan GB (2008) Forests and climate change: forcings, feedbacks, and the climate benefits of forests. *Science*, **320**, 1444–1449.

Bondeau A, Smith PC, Zaehle S *et al*. (2007) Modelling the role of agriculture for the 20th century global carbon balance. *Global Change Biology*, **13**, 679–706.

Borma LS, da Rocha HR, Cabral OMR *et al*. (2009) Atmosphere and hydrological controls of the evapotranspiration over a floodplain forest in the Bananal Island region, Amazonia. *Journal of Geophysical Research*, **114**, G01003, doi: 10.1029/2007JG000641.

Brando PM, Nepstad D, Davidson EA, Trumbore SE, Ray D, Camargo P (2008) Drought effects on litterfall, wood production and belowground carbon cycling in an Amazon forest: results of a throughfall reduction experiment. *Philosophical Transactions of the Royal Society B*, **363**, 1839–1848.

Cavaleri MA, Oberbauer SF, Ryan MG (2008) Foliar and ecosystem respiration in an old-growth tropical rain forest. *Plant, Cell and Environment*, **31**, 473–483.

Collatz GJ, Ball JT, Grivet C, Berry JA (1991) Physiological and environmental regulation of stomatal conductance, photosynthesis and transpiration: a model that includes a laminar boundary layer. *Agricultural and Forest Meteorology*, **54**, 107–136.

Cowling SA, Shin Y (2006) Simulated ecosystem threshold responses to co-varying temperature, precipitation and atmospheric CO_2 within a region of Amazonia. *Global Ecology and Biogeography*, **15**, 533–566.

Cox PM, Betts RA, Collins M, Harris PP, Huntingford C, Jones CD (2004) Amazonian forest dieback under climate-carbon cycle projections for the 21st century. *Theoretical and Applied Climatology*, **78**, 137–156.

Cox PM, Harris PP, Huntingford C *et al*. (2008) Increasing risk of Amazonian drought due to decreasing aerosol pollution. *Nature*, **453**, 212–216.

Cox PM, Stephenson D (2007) A changing climate for prediction. *Science*, **317**, 207–208.

Cramer W, Bondeau A, Woodward FI *et al*. (2001) Global response of terrestrial ecosystem structure and function to CO_2 and climate change: results from six dynamic global vegetation models. *Global Change Biology*, **7**, 357–373.

da Rocha HR, Manzi AO, Cabral OMR *et al*. (2009) Patterns of water and heat flux across a biome gradient from tropical forest to savanna in Brazil. *Journal of Geophysical Research*, **114**, G00B12, doi: 10.1029/2007JG000640.

Dolman AJ, Gash JHC, Roberts J, Shuttleworth WJ (1991) Stomatal and surface conductance of tropical rainforest. *Agricultural and Forest Meteorology*, **54**, 303–318.

Farquhar GD, von Caemmerer S, Berry JA (1980) A biochemical model of photosynthetic CO_2 assimilation in leaves of C_3 plants. *Planta*, **149**, 78–90.

Friedlingstein P, Dufresne JL, Cox PM, Rayner P (2003) How positive is the feedback between climate change and the carbon cycle? *Tellus*, **55B**, 692–700.

Friend AD, Arneth A, Kiang NY *et al*. (2007) FLUXNET and modelling the global carbon cycle. *Global Change Biology*, **13**, 610–633.

Gerten D, Schaphoff S, Haberlandt U, Lucht W, Sitch S (2004) Terrestrial vegetation and water balance – hydrological evaluation of a dynamic global vegetation model. *Journal of Hydrology*, **286**, 249–270.

Grant RF, Hutyra LR, de Oliveira RC, Munger JW, Saleska SR, Wofsy SC (2009) Modeling the carbon balance of Amazonian rain forests: resolving ecological controls on net ecosystem productivity. *Ecological Monographs*, **79**, 445–463.

Hallgren WS, Pitman AJ (2000) The uncertainty in simulations by a Global Biome Model (BIOME3) to alternative parameter values. *Global Change Biology*, **6**, 483–495.

Hawkins E, Sutton R (2009) The potential to narrow uncertainty in regional climate predictions. *Bulletin of the American Meteorological Society*, **90**, 1095–1107.

Haxeltine A, Prentice IC (1996a) BIOME3: an equilibrium terrestrial biosphere model based on ecophysiological constraints, resource availability, and competition among plant functional types. *Global Biogeochemical Cycles*, **10**, 693–709.

Haxeltine A, Prentice IC (1996b) A general model for the light-use efficiency of primary production. *Functional Ecology*, **10**, 551–561.

Hickler T, Prentice IC, Smith B, Sykes MT, Zaehle S (2006) Implementing plant hydraulic architecture within the LPJ dynamic global vegetation model. *Global Ecology and Biogeography*, **15**, 567–577.

Houghton RA, Lawrence KT, Hackler JL, Brown S (2001) The spatial distribution of forest biomass in the Brazilian Amazon: a comparison of estimates. *Global Change Biology*, **7**, 731–746.

Huntingford C, Fisher RA, Mercado L *et al*. (2008) Towards quantifying uncertainty in predictions of Amazon 'dieback'. *Philosophical Transactions of the Royal Society B*, **363**, 1857–1864.

IPCC (2007) Climate change 2007: the physical basis. In: *Contribution of Working Group I to the Fourth Assessment Report of the IPCC* (eds Soloman S, Qin D, Manning M *et al*.), Cambridge University Press, Cambridge, UK.

Jones RN (2001) An environmental risk assessment/management framework for climate change impact assessments. *Natural Hazards*, **23**, 197–230.

Keeling CD, Whorf T (2005) *Trends: A Compendium of Data on Global Change*. Carbon dioxide Information Analysis Center, Oak Ridge National Laboratory, Oak Ridge, TN.

Kobayashi H, Dye DG (2005) Atmospheric conditions for monitoring the long-term vegetation dynamics in the Amazon using normalized difference vegetation index. *Remote Sensing of Environment*, **97**, 519–525.

Lapola DM, Oyama MD, Nobre CA (2009) Exploring the range of climate biome projections for tropical South America: the role of CO_2 fertilization and seasonality. *Global Biogeochemical Cycles*, **23**, GB3003, doi: 10.1029/2008GB003357.

Lenton TM, Held H, Kriegler E *et al*. (2008) Tipping elements in the Earth's climate system. *Proceedings of the National Academy of Sciences*, **105**, 1786–1793.

Li W, Fu R, Dickinson RE (2006) Rainfall and its seasonality over the Amazon in the 21st century as assessed by the coupled models for the IPCC AR4. *Journal of Geophysical Research*, **111**, D02111, doi: 10.1029/2005JD006355.

Li W, Fu R, Juarez RIN, Fernandes K (2008) Observed change of the standardized precipitation index, its potential cause and implications to future climate change in the Amazon region. *Philosophical Transactions of the Royal Society B*, **363**, 1767–1772.

Lloyd J, Taylor JA (1994) On the temperature dependence of soil respiration. *Functional Ecology*, **8**, 315–323.

Malhi Y, Aragão LEOC, Galbraith D *et al*. (2009a) Exploring the likelihood and mechanism of a climate-change-induced dieback of the Amazon rainforest. *Proceedings of the National Academy of Sciences*, doi: 10.1073/pnas.0804619106.

Malhi Y, Aragão LEOC, Metcalfe DB *et al*. (2009b) Comprehensive assessment of carbon productivity, allocation and storage in three Amazonian forests. *Global Change Biology*, **15**, 1255–1274.

Malhi Y, Roberts JT, Betts RA, Killeen T, Li W, Nobre C (2008) Climate change, deforestation, and the fate of the Amazon. *Science*, **319**, 169–172.

Malhi Y, Wood D, Baker T *et al*. (2006) The regional variation of aboveground live biomass in old-growth Amazonian forests. *Global Change Biology*, **12**, 1107–1138.

McKay M, Beckman R, Conover W (1979) A comparison of three methods of selecting values of input variables in the analysis of output from a computer code. *Technometrics*, **21**, 239–245.

Nakicenovic N (Ed.) (2000) *Special Report on Emission Scenarios*. Intergovernmental Panel on Climate Change, Geneva, Switzerland.

Nepstad D, Stickler CM, Soares-Filho B (2008) Interactions among Amazon land use, forests, and climate: prospects for a near-term forest tipping point. *Philosophical Transactions of the Royal Society B*, **363**, 1737–1746.

Nepstad D, Tohver IM, Ray D, Moutinho P, Cardinot G (2007) Mortality of large trees and lianas following experimental drought in an Amazon forest. *Ecology*, **88**, 2259–2269.

New M, Lister D, Hulme M, Makin I (2002) A high-resolution data set of surface climate over global land areas. *Climate Research*, **21**, 1–25.

Österle H, Gerstengarbe FW, Werner PC (2003) Homogenisierung und Aktualisierung des Klimadatensatzes der Climate Research Unit der Universität of East Anglia, Norwich. *Terra Nostra*, **6**, 326–329.

Phillips OL, Malhi Y, Vinceti B *et al*. (2002) Changes in growth of tropical forests: evaluating potential biases. *Ecological Applications*, **12**, 576–587.

Poulter B, Aragao L, Heinke J *et al*. (in press) Net biome production of the Amazon Basin in the 21st century, *Global Change Biology*, doi: 10.1111/j.1365-2486.2009.02064.x.

Poulter B, Cramer W (2009) Satellite remote sensing of tropical forest canopies and their seasonal dynamics. *International Journal of Remote Sensing*, **30**, 6575–6590.

Poulter B, Heyder U, Cramer W (2009) Modelling the sensitivity of the seasonal cycle of GPP to dynamic LAI and soil depths in tropical rainforests. *Ecosystems*, **12**, 517–533.

Prentice IC, Bondeau A, Cramer W *et al*. (2007) Dynamic global vegetation modeling: quantifying terrestrial ecosystem responses to large-scale environmental change. In: *Terrestrial Ecosystems in a Changing World* (eds Canadell P, Pataki DE, Pitelka LF), pp. 175–192. Springer-Verlag, Berlin, Heidelberg, Denmark.

Raddatz TJ, Reick CH, Knorr W *et al*. (2007) Will the tropical land biosphere dominate the climate-carbon cycle feedback during the twenty-first century? *Climate Dynamics*, **29**, 565–574.

Raupach MR, Marland G, Ciais P *et al*. (2007) Global and regional drivers of accelerating CO_2 emissions. *Proceedings of the National Academy of Sciences*, **104**, 10288–10293.

Reich PB (1995) Phenology of tropical forests: patterns, causes, and consequences. *Canadian Journal of Botany*, **73**, 164–174.

Reichler T, Kim I (2008) How well do coupled models simulate today's climate? *American Meteorological Society*, **89**, 303–311.

Saatchi SS, Houghton RA, dos Santos Alvala RC, Soares JV, Yu Y (2007) Distribution of aboveground live biomass in the Amazon Basin. *Global Change Biology*, **13**, 816–837.

Salazar LF, Nobre CA, Oyama MD (2007) Climate change consequences on the biome distribution in tropical South America. *Geophysical Research Letters*, **34**, L09708, doi: 10.1029/2007GL029695.

Saleska SR, Miller SD, Matross DM *et al*. (2003) Carbon in Amazon forests: unexpected seasonal fluxes and disturbance-induced losses. *Science*, **302**, 1554–1558.

Saltelli A, Tarantola S (n.d.) Simlab 2.2 reference manual European commission – IPSC.

Scholze M, Knorr W, Arnell NW, Prentice IC (2006) A climate-change risk analysis for world ecosystems. *Proceedings of the National Academy of Sciences*, **103**, 13116–13120.

Shuttleworth WJ (1988) Evaporation from Amazonian rainforest. *Proceedings of the Royal Society of London*, **233**, 321–346.

Sitch S, Huntingford C, Gedney N *et al*. (2008) Evaluation of the terrestrial carbon cycle, future plant geography and climate-carbon cycle feedbacks using five Dynamic Global Vegetation Models (DGVMs). *Global Change Biology*, **14**, 2015–2039.

Sitch S, Smith B, Prentice IC *et al*. (2003) Evaluation of ecosystem dynamics, plant geography and terrestrial carbon cycling in the LPJ dynamic global vegetation model. *Global Change Biology*, **9**, 161–185.

Soares-Filho BS, Nepstad DC, Curran LM *et al*. (2006) Modelling conservation in the Amazon basin. *Nature*, **440**, 520–523.

Thonicke K, Venevsky S, Sitch S, Cramer W (2001) The role of fire disturbance for global vegetation dynamics: coupling fire into a Dynamic Global Vegetation Model. *Global Ecology and Biogeography*, **10**, 661–677.

Trudinger CM, Raupach MR, Rayner PJ *et al*. (2007) OptIC project: an intercomparison of optimization techniques for parameter estimation in terrestrial biogeochemical models. *Journal of Geophysical Research*, **112**, 602027, doi: 10.1029/2006JG000367.

Walker R, Moore NJ, Arima E *et al*. (2009) Protecting the Amazon with protected areas. *Proceedings of the National Academy of Sciences*, **106**, 10582–10586.

Werth D, Avissar R (2004) The regional evapotranspiration of the Amazon. *Journal of Hydrometeorology*, **5**, 100–109.

Wramneby A, Smith B, Zaehle S, Sykes MT (2008) Parameter uncertainties in the modelling of vegetation dynamics – Effects on tree community structure and ecosystem functioning in European forest biomes. *Ecological Modelling*, **216**, 277–290.

Xu C, Gertner GZ, Scheller RM (2009) Uncertainties in the response of a forest landscape to global climatic change. *Global Change Biology*, **15**, 116–131.

Zaehle S, Bondeau A, Carter TR *et al*. (2007) Projected changes in terrestrial carbon storage in Europe under climate and land-use change 1990–2100. *Ecosystems*, **10**, 380–401.

Zaehle S, Sitch S, Smith B, Hattermann F (2005) Effects of parameter uncertainty on the modeling of terrestrial biosphere dynamics. *Global Biogeochemical Cycles*, **19**, GB3020, doi: 3010.1029/2004GB002395.

Zobler L (1986) *A world soil file for global climate modeling*. NASA Technical Memorandum, 32 pp.

Supporting Information

Additional Supporting Information may be found in the online version of this article:

Figure S1. Simulated and measured gross ecosystem production (*GEP*) for the 6 flux tower sites. Confidence intervals are generated from the 1000 parameter set combinations and following simulations.
Figure S2. Simulated and measured ecosystem respiration (*Reco*) for the 6 flux tower sites. Confidence intervals are generated from the 1000 parameter set combinations and following simulations.
Figure S3. Spatial pattern of changes in soil carbon from 1981/00 mean reference period and 2081–2098 projection for all 8 climate models (SRES A2 emissions storyline).
Figure S4. Spatial pattern of ranked partial correlation coefficients (RPCC) for all parameters used in full Basin-wide simulations. The first column show the changes in soil carbon stocks between 2001/10 reference period and 2091/98 projection period for the standard parameter set (Std), the average of all parameter sets (Avg), and the standard deviation of soil carbon changes for all parameter sets (stdv). The first row corresponds to parameters related to carbon allocation, the second row for photosynthesis, and the third row contains parameters related to water use. The RPCC correlations are shown for the Hadley CM3 and GISS ER climate projections.
Figure S5. Spatial pattern of ranked partial correlation coefficients (RPCC) for all parameters used in full Basin-wide simulations. The first column show the changes in tropical evergreen cover between 2001/10 reference period and 2091/98 projection period for the standard parameter set (Std), the average of all parameter sets (Avg), and the standard deviation of tropical evergreen cover changes for all parameter sets (stdv). The first row corresponds to parameters related to carbon allocation, the second row for photosynthesis, and the third row contains parameters related to water use. The RPCC correlations are shown for the Hadley CM3 and GISS ER climate projections.
Table S1. List of parameters, original value, and parameter ranges, used in flux site simulations and Basin-wide simulations (boldfaced).
Table S2. Ranked partial correlation coefficients for individual flux sites (fulfilling criteria of being greater than a value of 0.2). The sites are ordered from left to right in terms of dry season length. A positive correlation indicates that variability in vegetation carbon storage is positively correlated with changes in the parameter value. These parameters were selected for the full Basin-wide simulation parameter set.
Table S3. Ranked partial correlation coefficients for individual flux sites (fulfilling criteria of being greater than a value of 0.2). The sites are ordered from left to right in terms of dry season length. A positive correlation indicates that variability in soil carbon storage is positively correlated with changes in the parameter value. These parameters were selected for the full Basin-wide simulation parameter set.
Table S4. Ranked partial correlation coefficients for individual flux sites (fulfilling criteria of being greater than a value of 0.2). The sites are ordered from left to right in terms of dry season length. A positive correlation indicates that variability in annual GPP storage is positively correlated with changes in the parameter value. These parameters were selected for the full Basin-wide simulation parameter set.
Table S5. Ranked partial correlation coefficients for individual flux sites (fulfilling criteria of being greater than a value of 0.2). The sites are ordered from left to right in terms of dry season length. A positive correlation indicates that variability in tropical evergreen cover is positively correlated with changes in the parameter value. These parameters were selected for the full Basin-wide simulation parameter set.
Table S6. Ranked partial correlation coefficients for changes in soil carbon (1981/00 to 2081/98) for the Eastern and Western Amazon Basin. The RPCC values must be interpreted in the context of the directly change of soil carbon for each model, these are illustrated in Fig. S3.
Table S7. Ranked partial correlation coefficients for changes in tropical evergreen cover (1981/00 to 2081/98) for the Eastern and Western Amazon Basin. The RPCC values must be interpreted in the context of the directly change of tropical evergreen cover for each model, these are illustrated in Fig. 5a.